

Transformation of P-S to P-P seismic data

Wai-kin Chan and Robert R. Stewart

ABSTRACT

Conventional converted-wave processing requires special algorithms to account for the P-S asymmetric move-out in the CMP domain. Two techniques, asymmetric move-out correction (ASMO) and average V_p/V_s value analysis by simulated annealing are proposed to correct for this asymmetric move-out behavior and transform the P-S data into P-P, so that normal P-wave processing algorithms can be followed. The synthetic example presented here shows some promising results.

INTRODUCTION

A more complete recording of the seismic experiment requires measurement of three components of the received waves. From these 3-C measurements we can attempt to improve P-wave sections and create independent converted-wave (P-S) images. Jointly interpreting P-P and P-S sections can significantly improve the description of the geological section and reservoir rocks. To facilitate this ultimate interpretation though, we need to make P-S data easily correlative to P-P data. To do this, we would like to have both sections in P-P time (or depth). We would also like to be able to use the existing tools of P-P processing and have this whole procedure take minimal time.

We propose to solve these problems by transforming P-S data to P-P times. This will reposition the P-S data (with their asymmetric ray paths and gathers) to look like symmetric P-P data. We can then use many of the efficient conventional processes such as CMP binning and DMO. This technique is based on a new asymmetric movout correction (ASMO) and V_p/V_s value analysis.

THEORY OF ASMO

The method of the ASMO starts from the downward continuation of the received wavefield, with P-wave velocity, to a depth increment. The P-wave travel-times from the shot to the depth points are calculated. The time samples of the downward continuation wavefield that corresponding to the calculated travel-times are then upward continued with S-wave velocity. This procedure is repeated for all depth increments and the output of the transformation is the summation of all the upward continuation of S-wavefield. Let $S(x, z=0, t)$ denote the recorded P-S shot gather at the Earth's surface, then the corresponding pseudo P-P shot gather, $P(x, z=0, t)$ is given by

$$P(x, 0, t) = \sum_z U_z^{Vs} [D_z^{Vp} [S(x, 0, t)] \delta(t - t_d(x, y))] \quad (1)$$

where U_z^{Vs} is the upward continuation operator from z to the surface with V_s velocity,

D_z^{Vp} is the downward continuation operator from the surface to z with V_p velocity

t_d is the P-wave travel-times from the shot to the depth points (x, z) ,

δ is the Dirac delta function.

In essence, the receivers are downward continued with S-wave velocity field to a cer-

tain level, then upward continued with P-wave velocity field to the surface as shown in Figure 2. We note that during the process, the amplitudes of the P-S reflections are mapped from P-S times and positions into the P-P configuration. If the pseudo P-P shot is migrated with the P-wave velocity, the amplitude of the migrated shot image is simply the P-S reflectivity that could also be obtained from migration of the same P-S shot. Also the angle of incidence corresponding to each offset on the pseudo P-P data are the same as the P-P data having the same offset. After the transformation, note that the pseudo P-P shot gather has greater lateral offset than the original P-S data (Figure 2), which is due to the fact that the P-S conversion points are away from the shot. The ASMO procedure can also apply to the receiver domain, which results in lessening the offsets. However, in this receiver domain, the ASMO faces less statics problem, as the P-wave shot statics can be applied first. The residual receiver statics can then be solved in the CMP domain, as usual. If both P- and S- velocities have small lateral variation and the V_p/V_s values vary smoothly, the RMS velocities of P and S can be used rather than the interval velocities for the transformation. In this paper, RMS velocity field is used for the ASMO.

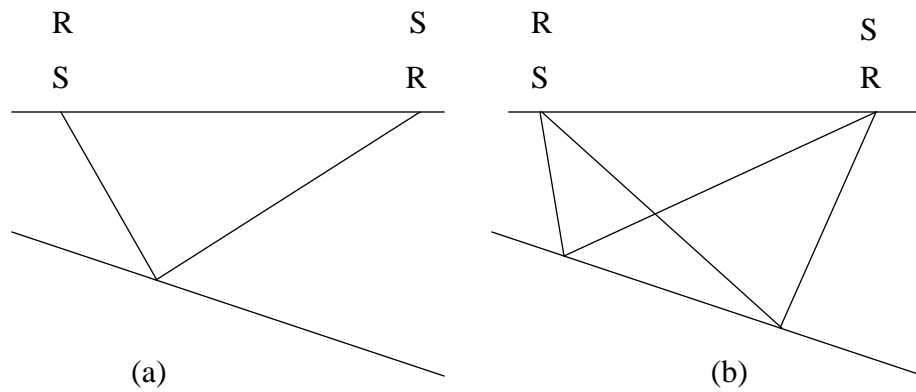


Fig. 1. (a) By exchanging source (S) and receiver (R) positions, the ray paths remain the same for P-P or S-S reflections, therefore the travel-time is symmetric with respect to the source-receiver mid-point. (b) By exchanging source (S) and receiver (R) positions, the P-S reflections follow different paths, with the conversions away from the shot (S), therefore the travel-times are different and the symmetry breaks down with respect to the source-receiver mid-point.

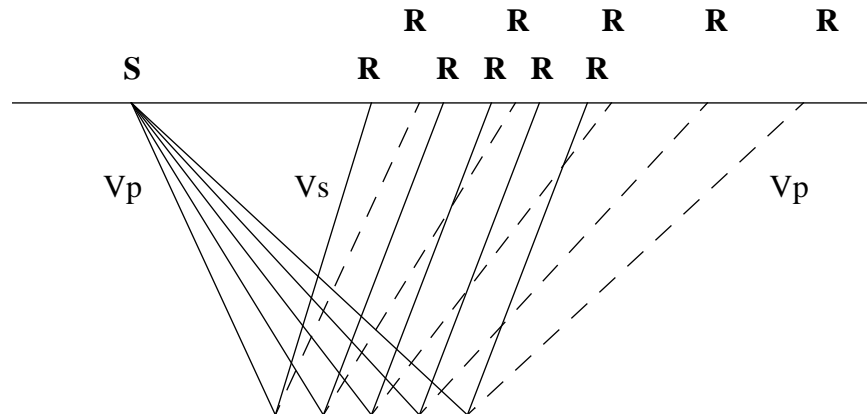


Fig. 2. The ASMO can be visualized as the receivers being downward continued with S velocity

(Vs) to a certain depth, followed by upward continuation to the surface with P velocity (Vp).

Vp/Vs analysis

In the above method, it is assumed that the background RMS velocities for both P and S are known. In general, both velocity fields can be extracted from the velocity analysis during the P-P and the P-S processing. However, if after the transformation, the events on the pseudo P-P data need to be tied with that on the real P-P data, then these velocities may not be accurate enough. Consider a simple uniform layer, shown in Figure 3, 3 km thick and with $V_p = 3000$ m/s, $V_s = 1500$ m/s. The two-way vertical P-P and P-S travel-times for this model are 2 seconds and 3 seconds respectively. Assuming that there is only -3% relative error in the S velocity giving $V_s = 1455$ m/s and $V_p/V_s = 2.06$. The event at 3 seconds two-way P-S time, now maps to 1.96 seconds two-way P-P time giving -40 ms in error. If the dominant frequency of the wavelet in the P-P data is 30 Hz. This 40 ms error translates into more than a dominant wavelength of the wavelet. We conclude that the average Vp/Vs ratio in depth from the correlation of the events on the P-P and the P-S data, especially for the latter events, is much sensitive than the one obtained from the normal velocity analysis, which has more error for the later events. Therefore, tying the events between P-P and P-S data can provide excellent estimation of the average Vp/Vs ratios and these ratios can be used for the purpose of the P-S transformation. In the next section, it will be shown that simulated annealing technique can be incorporated to correlate events between P-P and P-S automatically and to obtain the variable average Vp/Vs ratios in the time and space domains. Once these average Vp/Vs ratios are obtained, they can be converted into interval Vp/Vs ratios, for example by analyzing the P-P and P-S interval times between a major geological event.

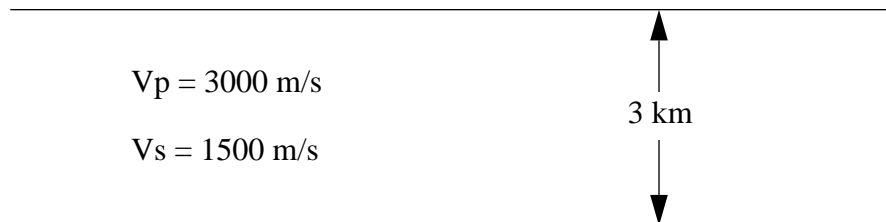


Fig. 3. Consider a 3km thick uniform layer with $V_p=3000$ m/s and $V_s=1500$ ms. The P-P and the P-S two-way vertical travel-times of the model are 2 seconds and 3 seconds respectively. If the event at 3 seconds P-S time is compressed to P-P time with $V_p=3000$ m/s and $V_s=1455$ m/s, the resulted P-P time will be at 1.96 seconds giving -40 ms error.

SIMULATED ANNEALING

Simulated annealing has long been used as a technique to solve global optimization problems in geophysics (Rothman, 1985, Sen and Stoffa, 1991, Chunduru et al., 1996, Jervis et al., 1996). Starting from an initial point, the algorithm takes a step and the optimization function is evaluated. It is different from other optimization techniques, like the nonlinear simplex (Rowan, 1990), that only accepts a favorable solution during each step. By accepting non-favorable solutions occasionally, based on Metropolis criteria, local optima can be escaped. As the optimization process proceeds, the step lengths decline, the chance of accepting non-favorable solutions decreases, and the algorithm closes in on the global optimum.

Correlation of events between P-P and P-S stack traces can be formulated as a global

optimization problem. The functional value to be optimized is the cross-correlation between the reference P-S trace and the stretched P-P trace, based on the current estimated average V_p/V_s values. When the proper V_p/V_s values applied on the stacked traces, the match between two traces reaches optimum, and hence it gives the largest cross-correlation value. This technique assumes that the P-S and P-P reflectivity are well correlated. If this is not true at some locations in time, the V_p/V_s values obtained at these locations are in error. However as it is the average V_p/V_s value, not the interval V_p/V_s value being sought, the errors should be localized.

The number of the average V_p/V_s values used in a trace is important. Fortunately, from the P-wave horizon velocity analysis, several key horizons or events are already identified in terms of P-wave two-way travel-times, and they can be used as control points for the V_p/V_s analysis. The V_p/V_s values among the control points are just linear interpolated, and the resulted V_p/V_s values become functions of P-wave travel times and CDP locations. To further stabilize the solution of the optimization, the match is first done on the low frequency version of the P-P and the P-S stack traces. The result of these V_p/V_s values is used as constrains for the final match between the original P-P and P-S traces.

ALTERNATIVE CONVERTED-WAVE PROCESSING

Figure 4 is the flow chart for the traditional converted-wave processing for the DMO stack, assuming anisotropy is not important and rotation analysis is not required. Figure 5 is the proposed flow chart for the same DMO stack. There are two main advantages of the alternative flow: First, interactive velocity analysis is avoided for the P-S data, and only the previously known P velocities are needed for different stacking purposes. Second, the normal P-wave processing flow can be used without the need for developing a special 3-D P-S DMO. The P-S flow is now considerably simplified.

NUMERICAL SYNTHETIC EXAMPLE

A finite-difference elastic modelling program (Cruse, pers. comm.) is used to simulate a 2D-2C survey with a point source. Figure 6 is the velocity-density model for the synthetic data. A total of 200 split-spread shots are generated. Each record contains 131 channels (including zero offset) on one side, and 100 channels on the other side. The station interval is 25 m and every station is shot. To simplify the multiple problem, the data are generated with no free-surface effects. Figures 7 and 8 are vertical and radial components of a shot at station 1200. Only 201 channels are shown. Scaling has been applied on both records and polarity reversal has been applied on the radial component. Figures 9 and 10 are P-P and P-S CMP gathers at station 1200 respectively. Note that the second layer reflection on the P-P CMP gather is symmetric with respect to the offset, but not in the P-S CMP gather. Figures 11 and 12 are P-P DMO stack and P-P prestack time migrated stack (Gardner et al., 1986; Canning, 1993). Figure 13 is asymptotic common conversion (ACCP) stack with V_p/V_s ratio of 2.

In the new flow, a constant V_p/V_s ratio of 1.8 is used for the transformation of the P-S shot gather into pseudo P-P shot gather. This is followed by DMO and stack. The pseudo P-P DMO stack is shown in Figure 14. Because of the wrong V_p/V_s ratio, the stack does not match the true DMO stack (Figure 11), in terms of the zero-offset times. However, after stretching the pseudo-section back to P-S time with the same V_p/V_s ratio used for the transformation, the resultant section (Figure 15) is very similar to the ACCP stack as shown in Figure 13. This suggests that a useful P-S DMO stack can be obtained in the new flow, perhaps with better V_p/V_s ratios.

The next step is to use simulated annealing technique to analysis the time and space variant V_p/V_s ratios. A selected subset of pseudo P-P DMO stack in P-S time (Figure 16) is used for reference traces for the correlation. In Figure 17, the corresponding true P-P DMO stack traces are stretched with the estimation of V_p/V_s ratios from the correlation analysis. Comparing between Figure 16 and Figure 17, it suggested the simulated annealing does obtain optimum V_p/V_s ratios for the match. These new estimated V_p/V_s ratios are used to update the transformation process. Figure 18 is the updated pseudo P-P shot gather. After the transformation, the largest offset changes from 3250 m to about 5000 m. Figures 19 and 20 show the limited offsets version of Figure 18 in shot and CMP domains. Figure 21 is the new pseudo P-P DMO stack, and it is in general agreement with the true P-P DMO stack (Figure 9). There are some mis-ties at around station 1950 for the last layer. The main reason is that the estimated V_p/V_s ratios are along the normal ray paths and the velocities used for the ASMO are along image ray paths. Because there is significant lateral velocity variation in that region, these two ray paths are different enough to give rise to the error. Figure 22 is the pseudo P-P DMO stack plotted in the P-S time. This also represents the P-S DMO stack. The pseudo P-P prestack gathers are also migrated with the P-P algorithm and the stack is shown in Figure 23. The receiver version of the ASMO was also tested. Figures 24 and 25 are the receiver gather at station 1194 and CMP gather at station 1200. The resultant pseudo P-P DMO stack is shown in Figure 26. It is similar to Figure 21, but it is nosier, especially on the top. This is due to the loss of offset after ASMO. This suggests that a top mute may be necessary after the receiver ASMO.

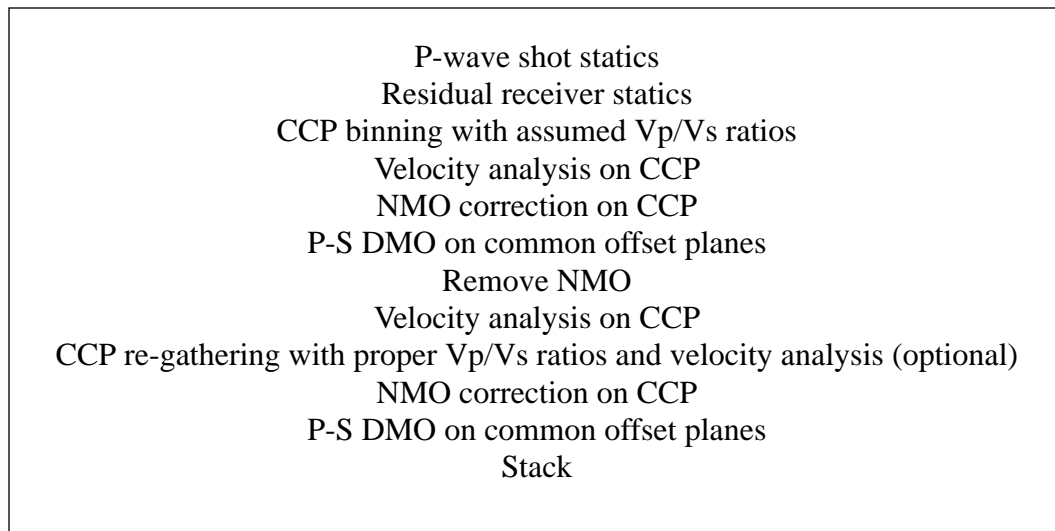


Fig. 4. The flow chart for the traditional converted-wave DMO stack.

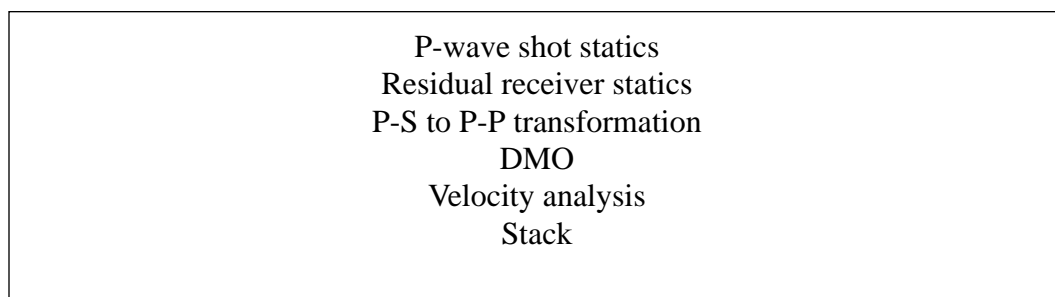


Fig. 5. The alternative flow chart for the converted-wave DMO stack

CONCLUSIONS

Two new techniques, ASMO and Vp/Vs analysis using simulated annealing have been discussed. It has been shown that these two techniques can be used together to transform the P-S data into P-P time and form an alternative processing flow for converted-waves. This eliminates the need for the P-S velocity analysis, and normal P-P processing algorithms can be followed. These techniques can be easily extended to 3-D geometries and special 3-D processing algorithms for P-S data, like 3-D P-S DMO can be avoided.

REFERENCES

Canning A., 1993, Organization and imaging of three-dimensional seismic reflection data before stack: Ph.D. thesis, Rice University.

Chundurur, R. K., Sen, M. K., and Stoffa, P. L., 1996, 2-D resistivity inversion using spline parameterization and simulated annealing: *Geophysics*, 61, 151-161.

Gardner, G. H. F., Wang, S. Y., Pan, N. D., and Zhang, Z., 1986, Dip-moveout and prestack imaging: *Ann. Mtg. Offshore Tech. Conf., Expanded Abstracts*, Vol. 2, 75-81.

Jervis, M., Sen, M. K., and Stoffa, P. L., 1996, Prestack migration velocity estimation using nonlinear methods: *Geophysics*, 61, 138-150.

Rowan, T., 1990, Functional stability analysis of numerical algorithms: Ph.D. thesis, Department of Computer Sciences, University of Texas at Austin.

Rothman, D. H., 1985, Nonlinear inversion, statistical mechanics, and residual statics estimation: *Geophysics*, 50, 2784-2796.

Sen, M. K., and Stoffa, P. L., 1991, Nonlinear one-dimensional seismic wave form inversion using simulated annealing: *Geophysics*, 56, 1624-1638.

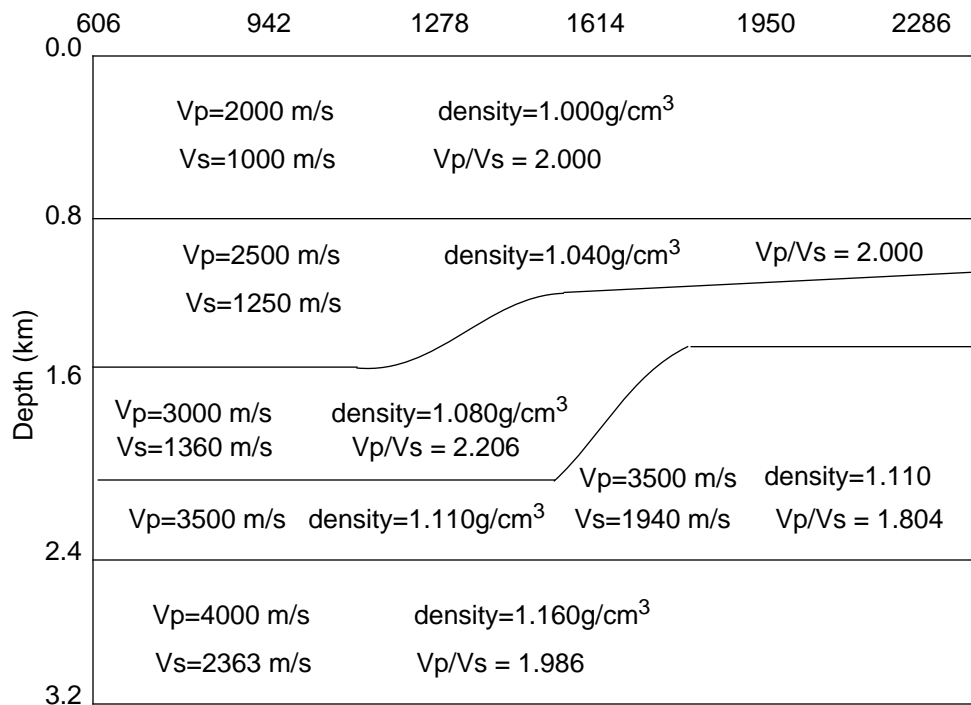


Fig. 6. Velocity-density depth model of the numerical synthetic example.

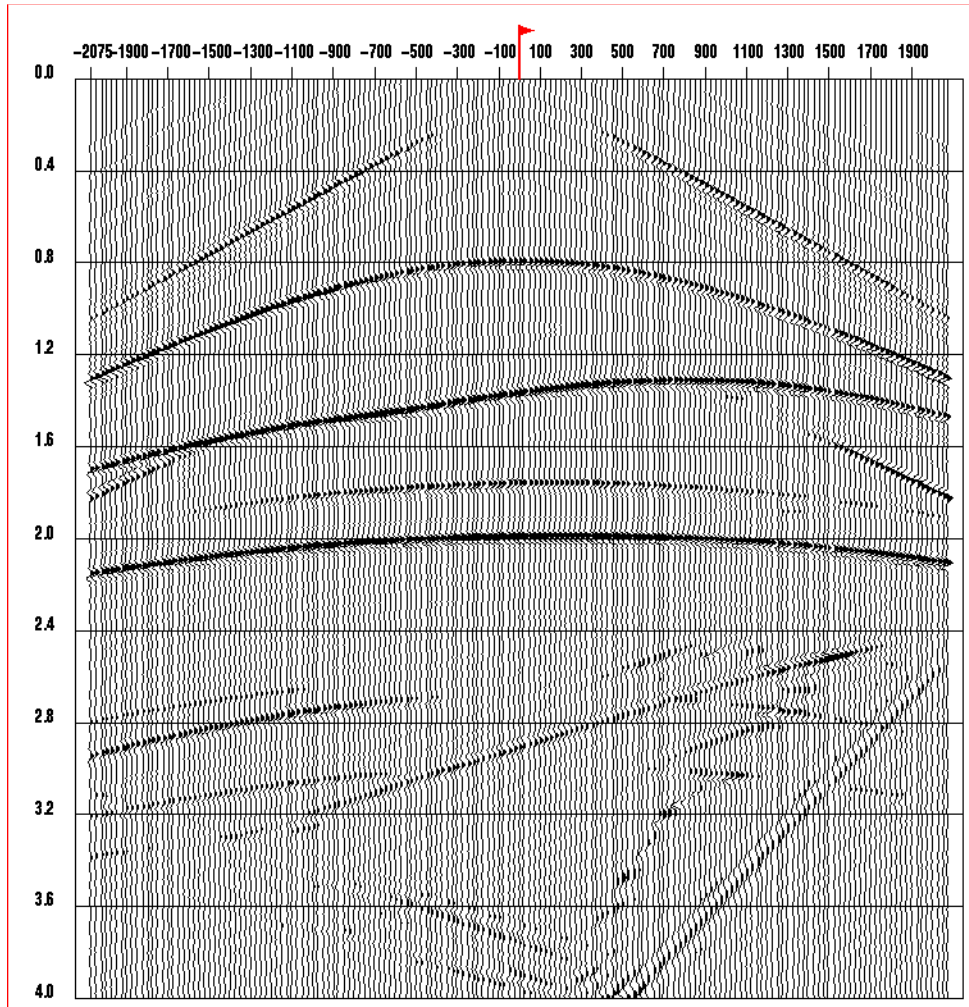


Fig. 7. Vertical component of a shot record at station 1200. The 4 primary P-P reflections are at 0.8 s, 1.3 s, 1.8 s and 2 s of zero offset times respectively. Scaling has been applied to the record.

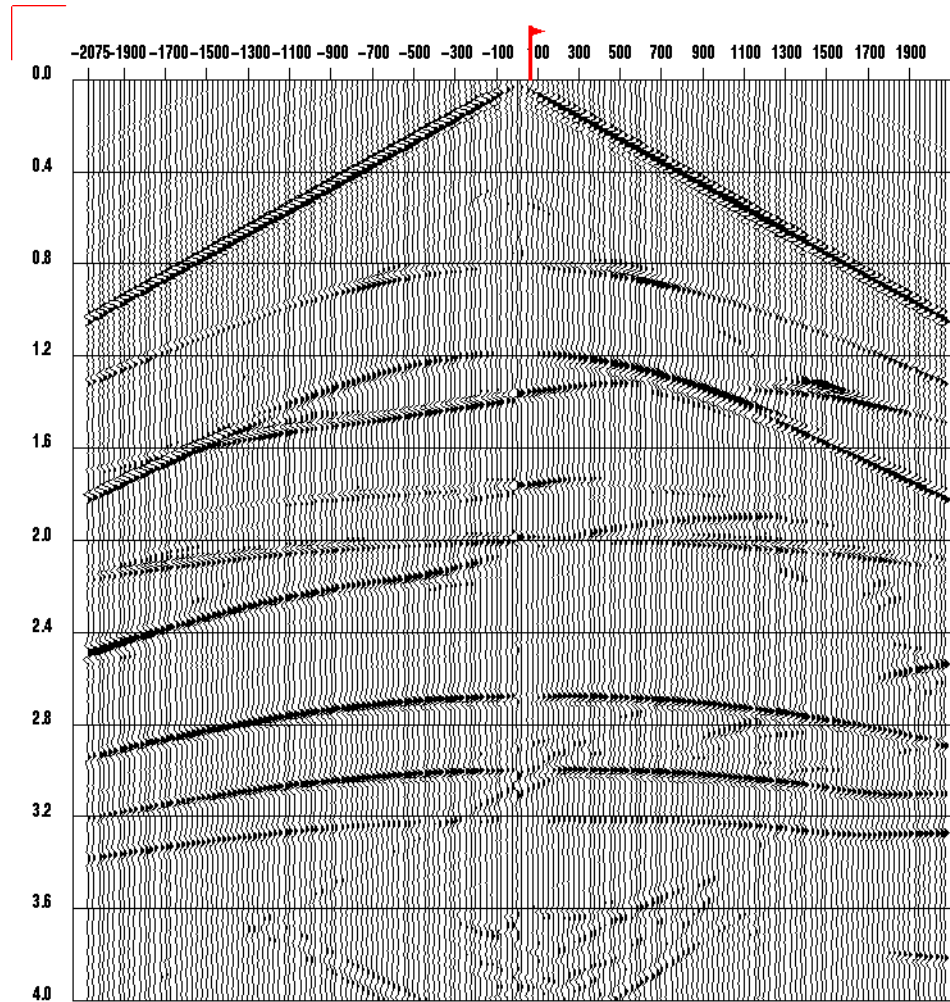


Fig. 8. Radial component of a shot record at station 1200. The 4 primary P-S reflections are at 1.2 s, 2.0 s, 2.7 s and 3 s of zero offset times respectively. Scaling and polarity reversal have been applied to the record.

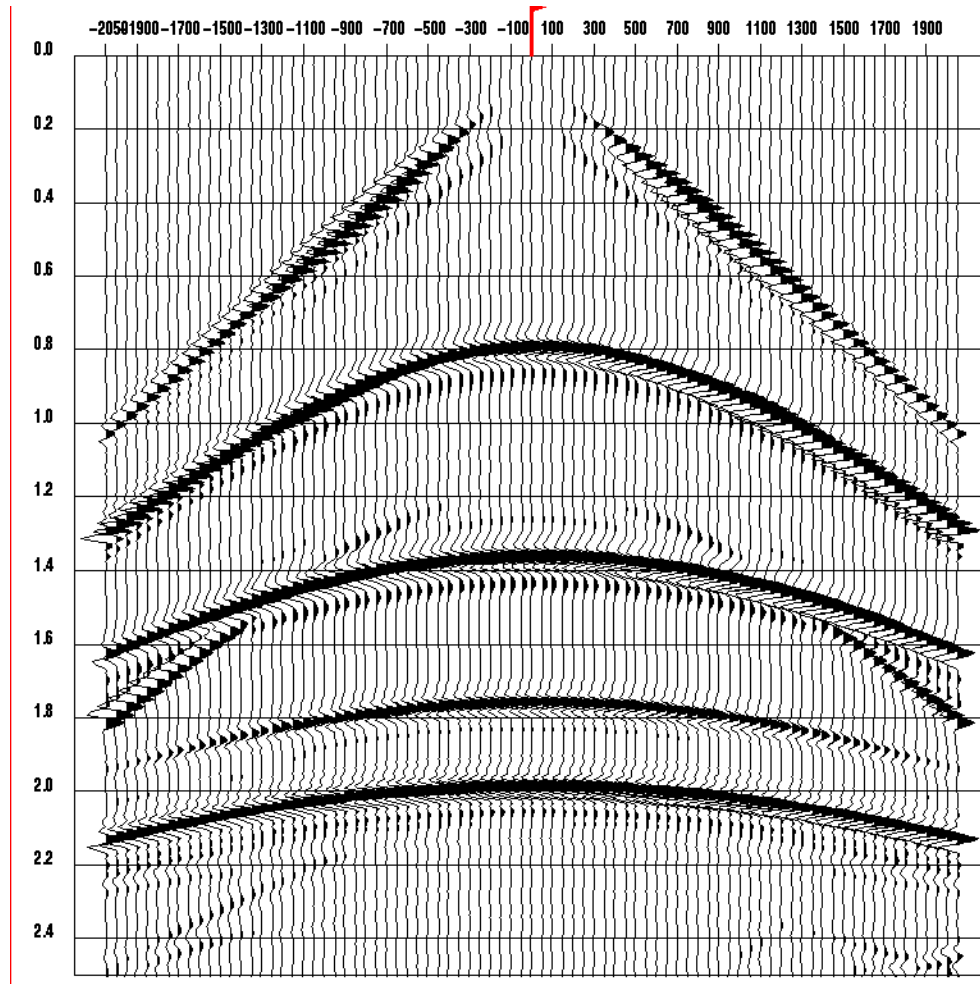


Fig. 9. A P-P CMP gather at station 1200. Note that the event at 1.35 seconds is symmetric with respect to the offset.

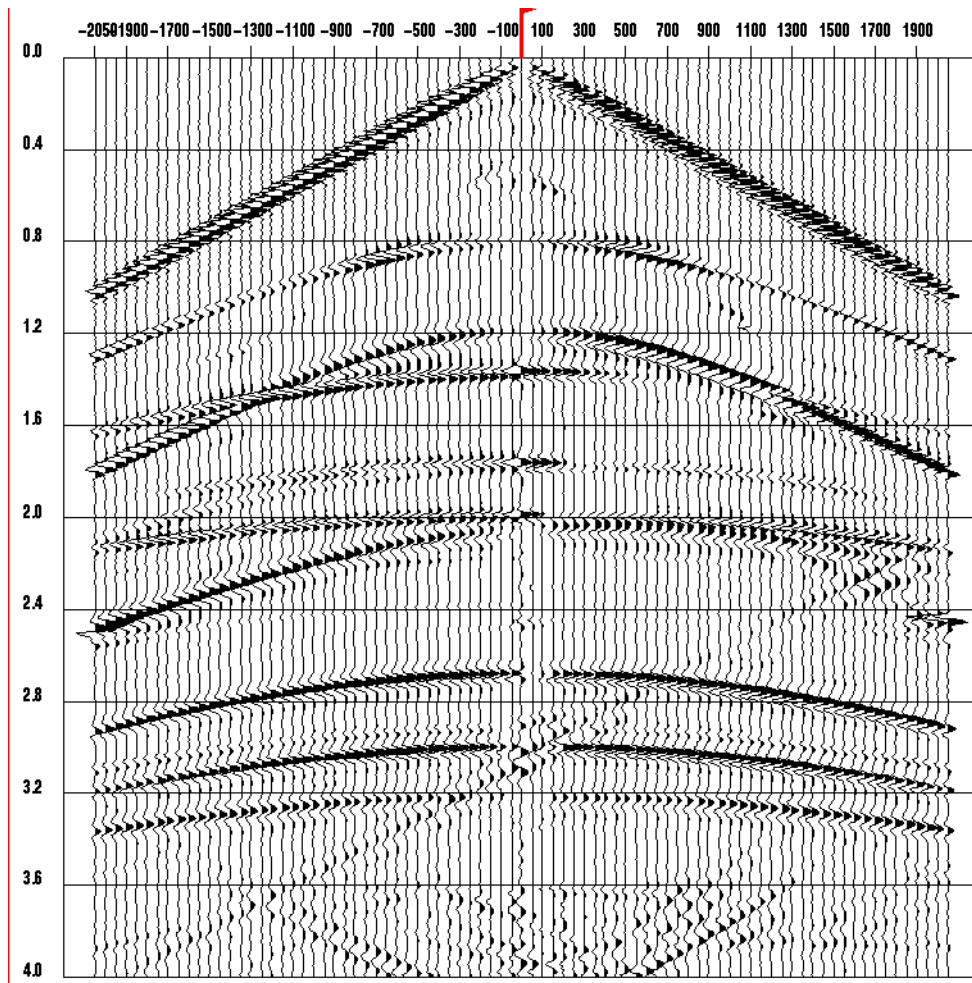


Fig. 10. A P-S CMP gather at station 1200. Note that the event at 2 seconds is asymmetric with respect to the offset.

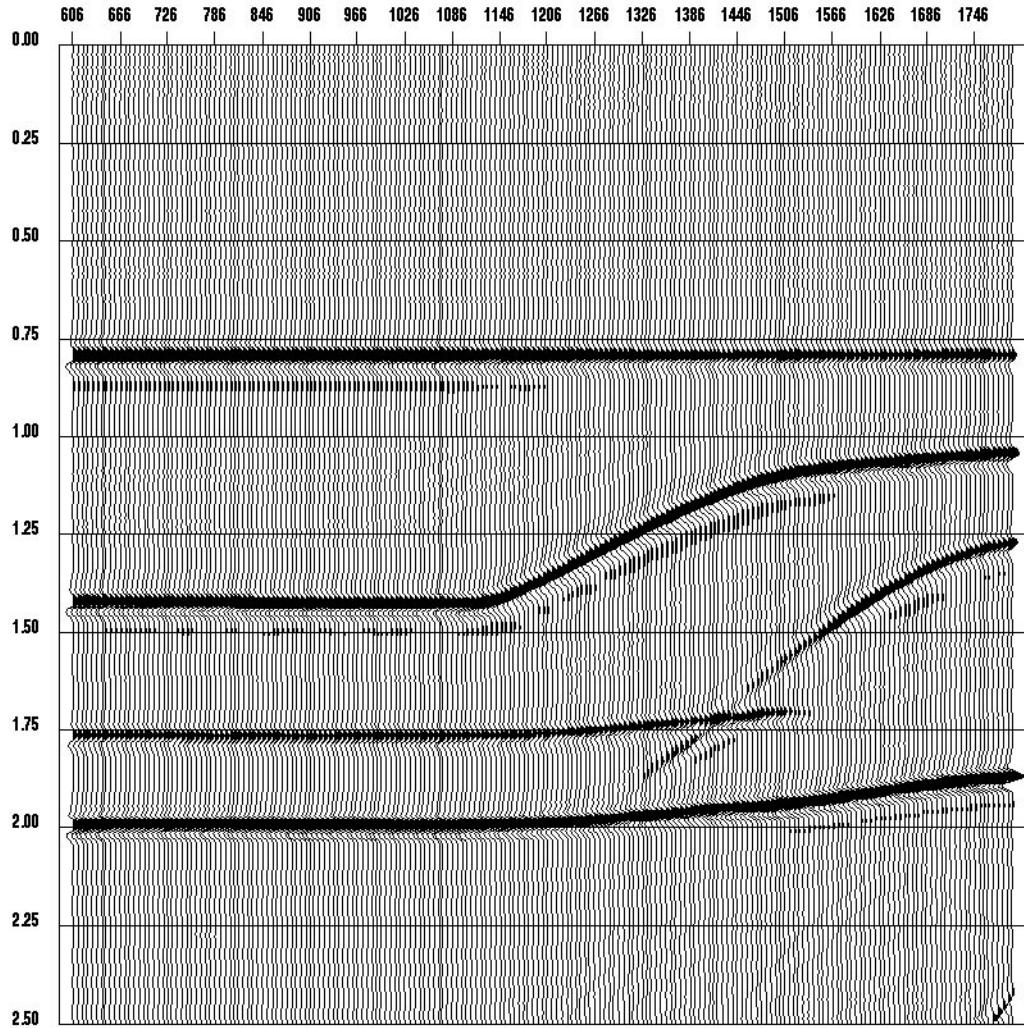


Fig. 11. P-P DMO stack.

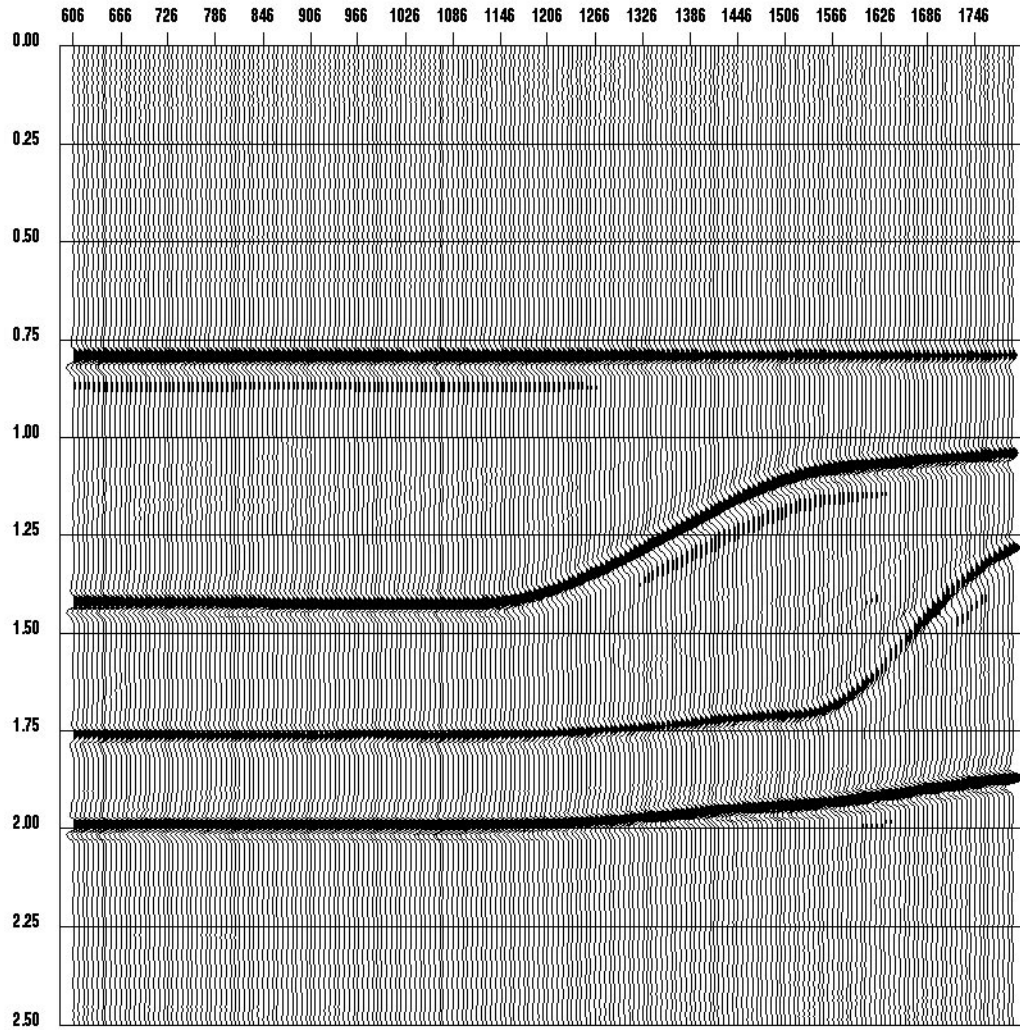


Fig. 12. P-P prestack time migrated stack.

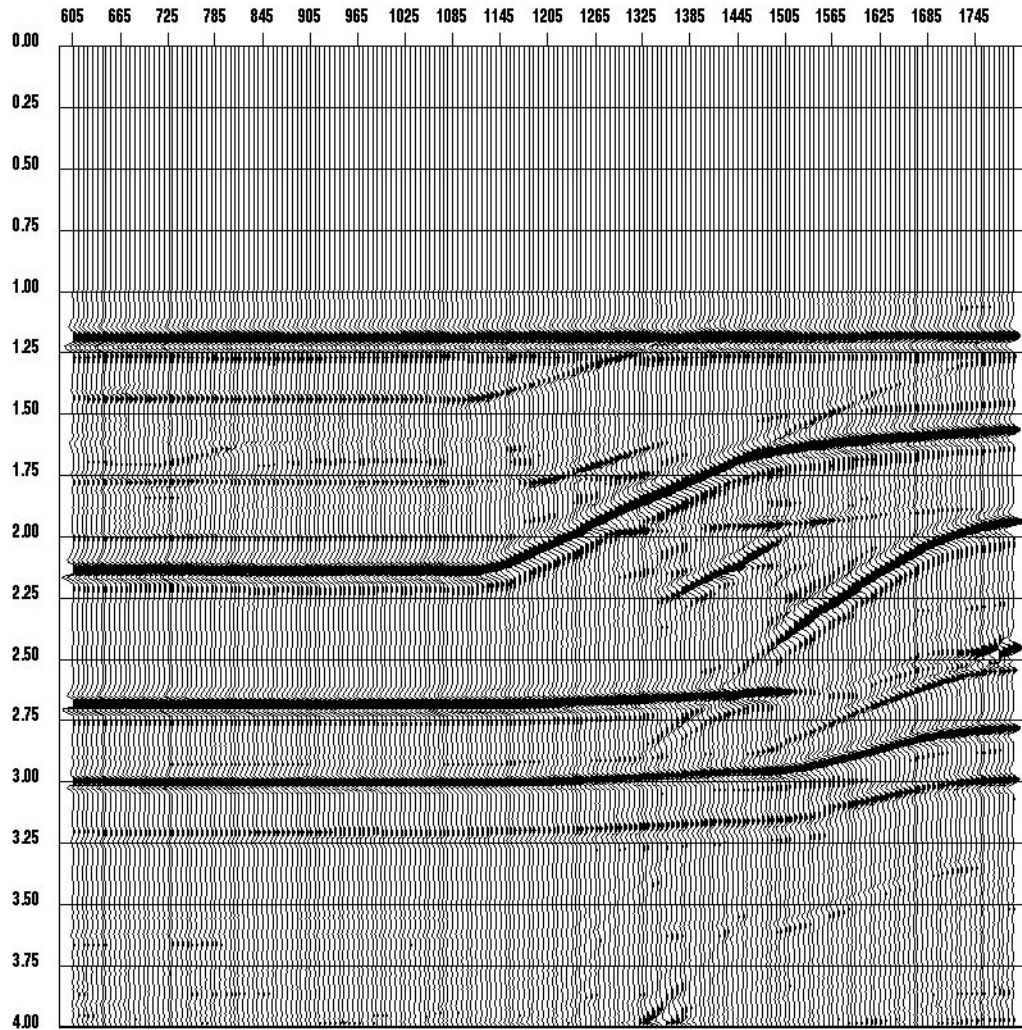


Fig. 13. Asymptotic common conversion point (ACCP) stack of P-S data with $V_p/V_s=2.0$.

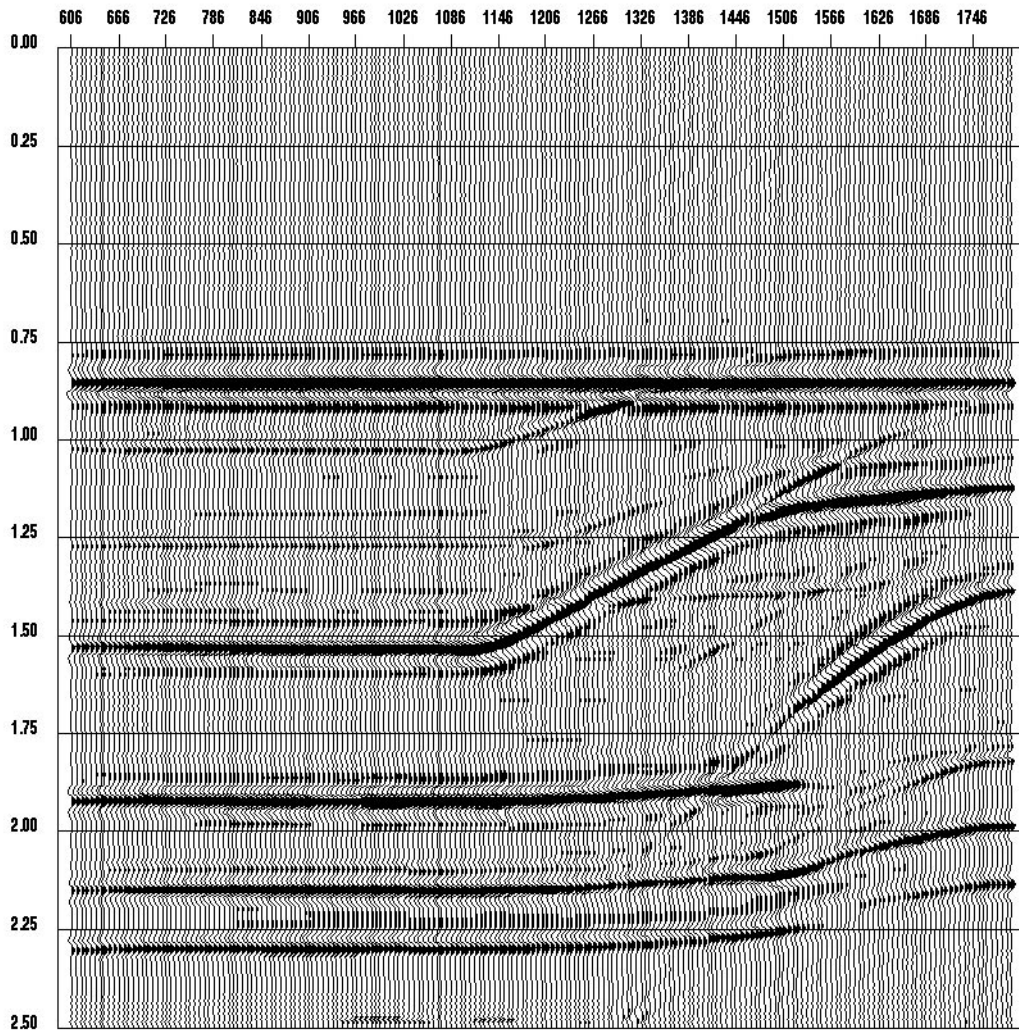


Fig. 14. Pseudo P-P DMO stack. A constant $V_p/V_s = 1.8$. is used for transformation. Note that the times of the events do not match with the true P-P DMO stack in Figure 9.

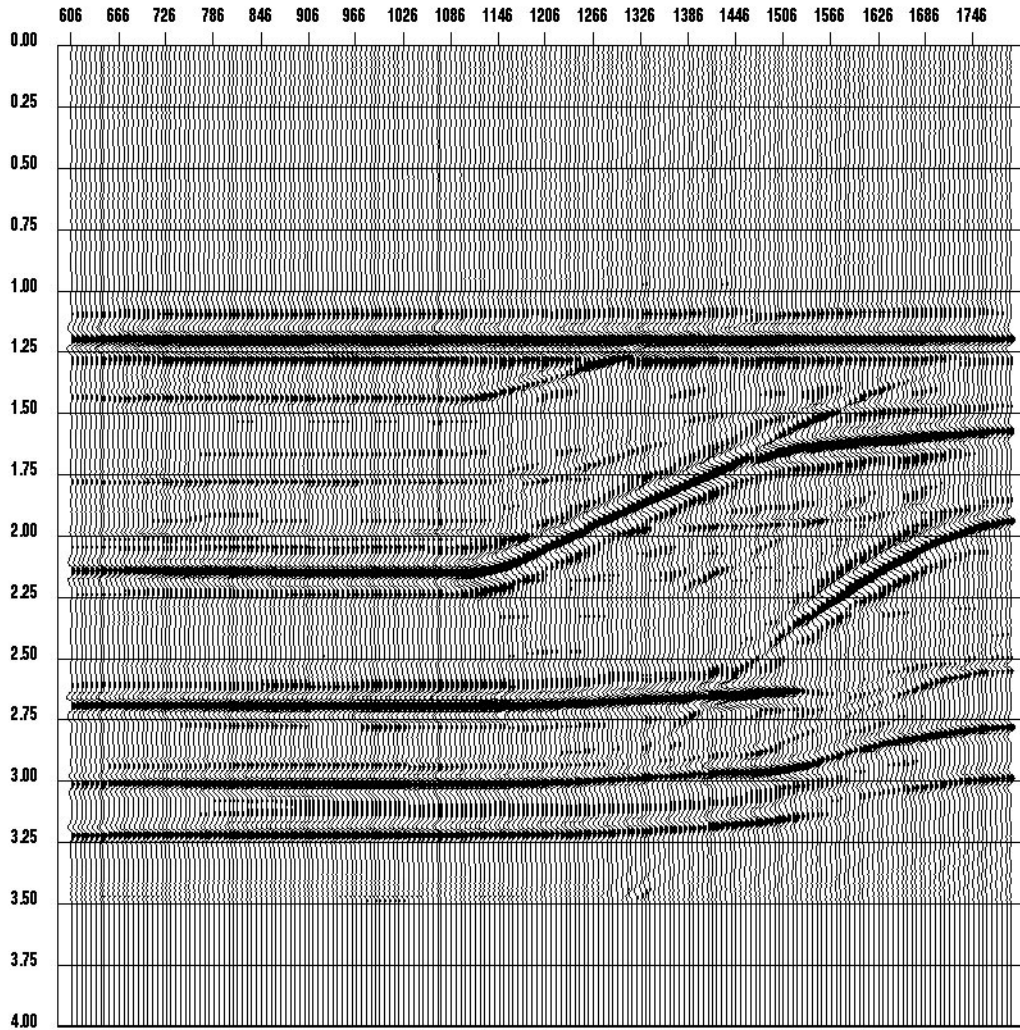


Fig. 15. The pseudo P-P DMO stack is vertically stretched in P-S time using $V_p/V_s=1.8$. The times of the events are similar to ACCP stack in Figure 11.

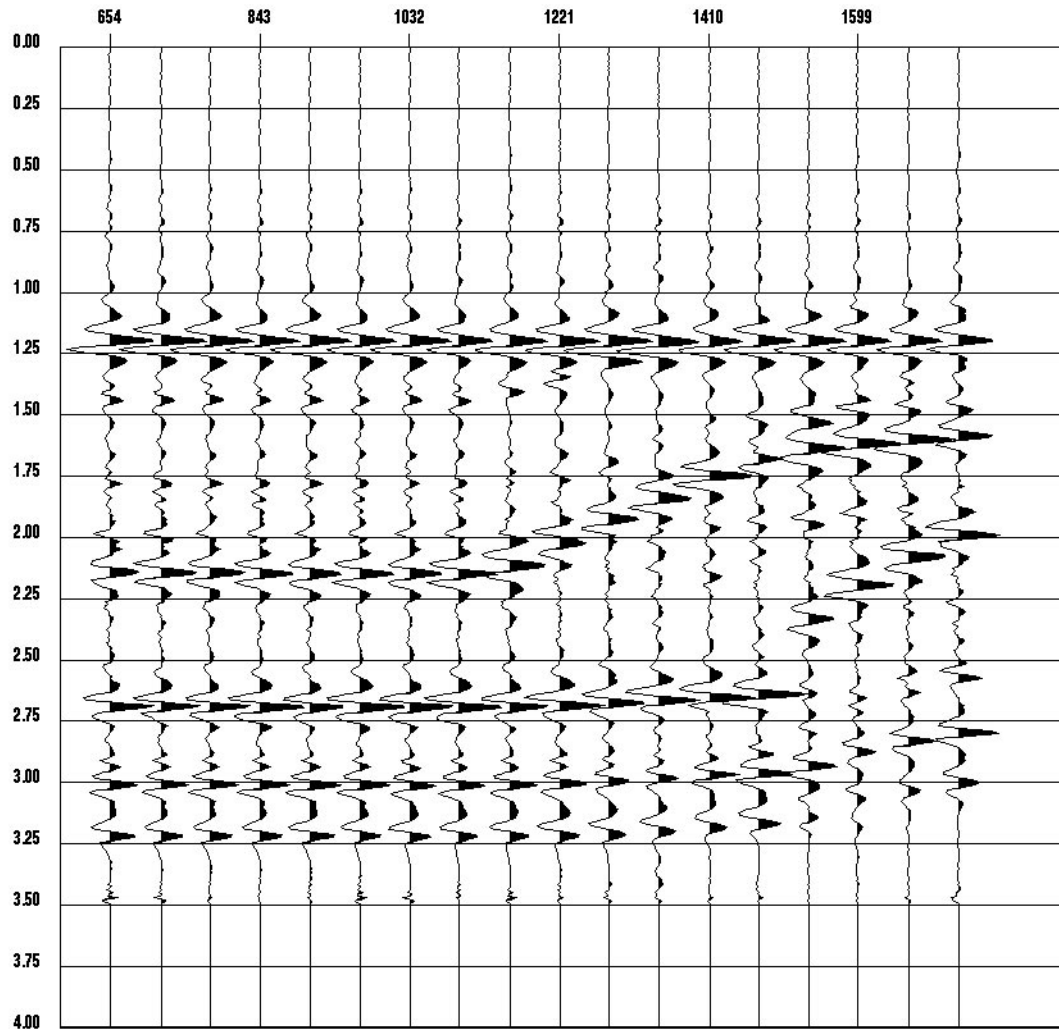


Fig. 16. A selected subset of pseudo P-P DMO stack in P-S time for correlation reference. This is used, together with the true P-P stack to estimate space-time variant V_p/V_s ratios.

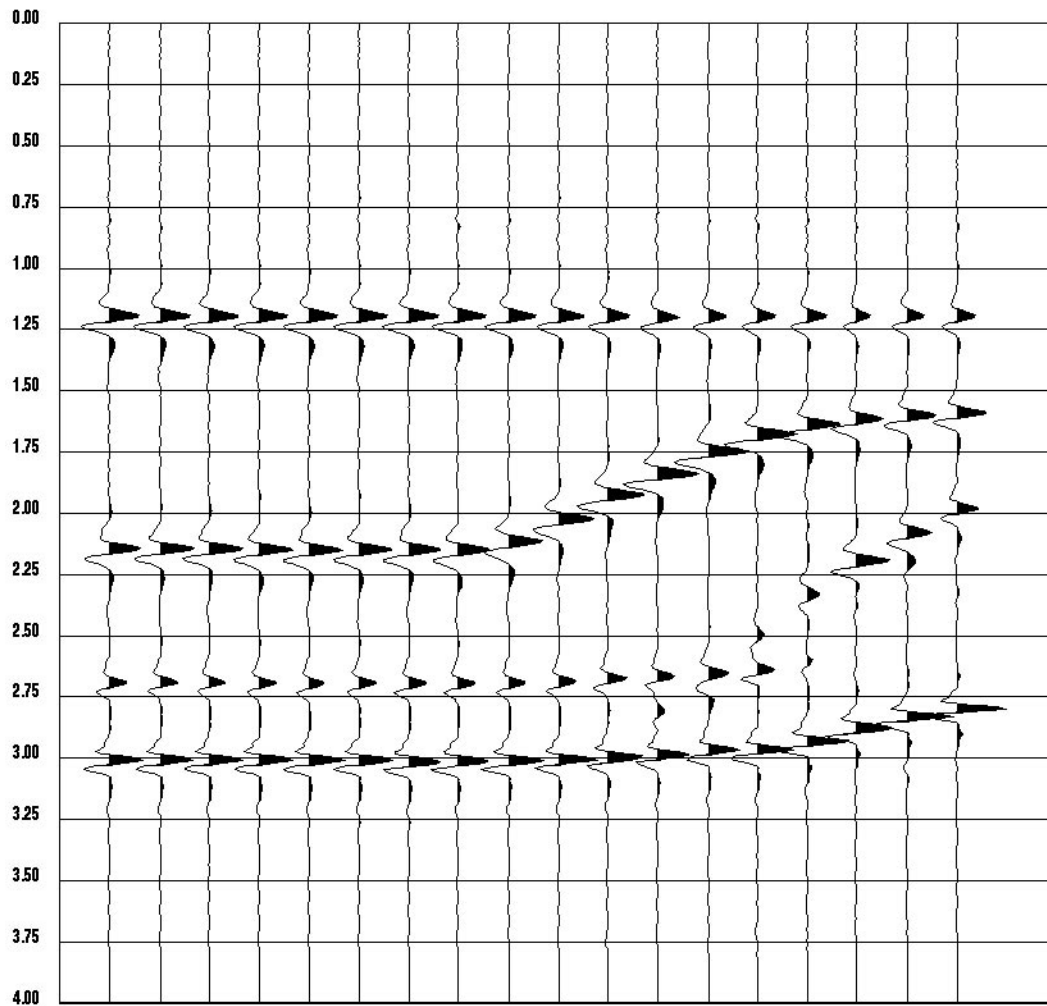


Fig. 17. The corresponding true P-P stack stretched in P-S time using the first estimated V_p/V_s ratios from the result of simulated annealing. The times of the events closely match those in Figure 16.

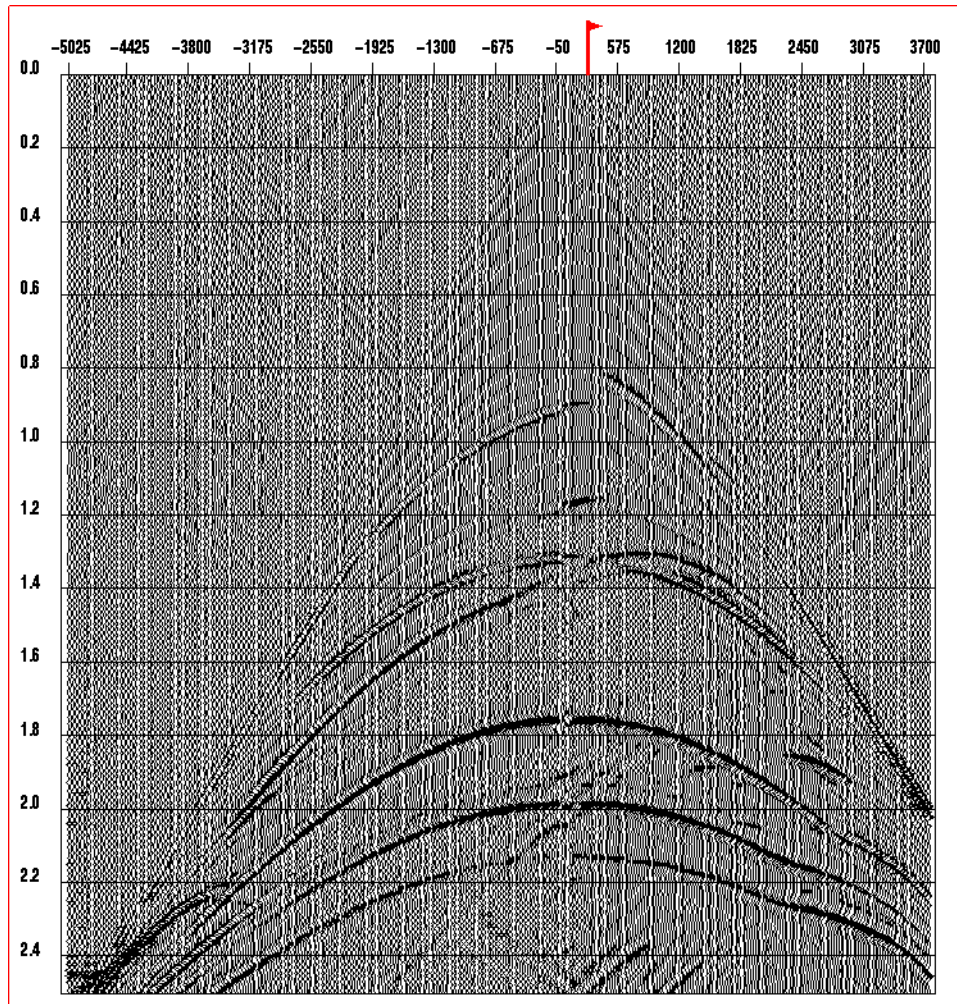


Fig. 18. The pseudo P-P pseudo shot gather at station 1200, using estimated V_p/V_s ratios.

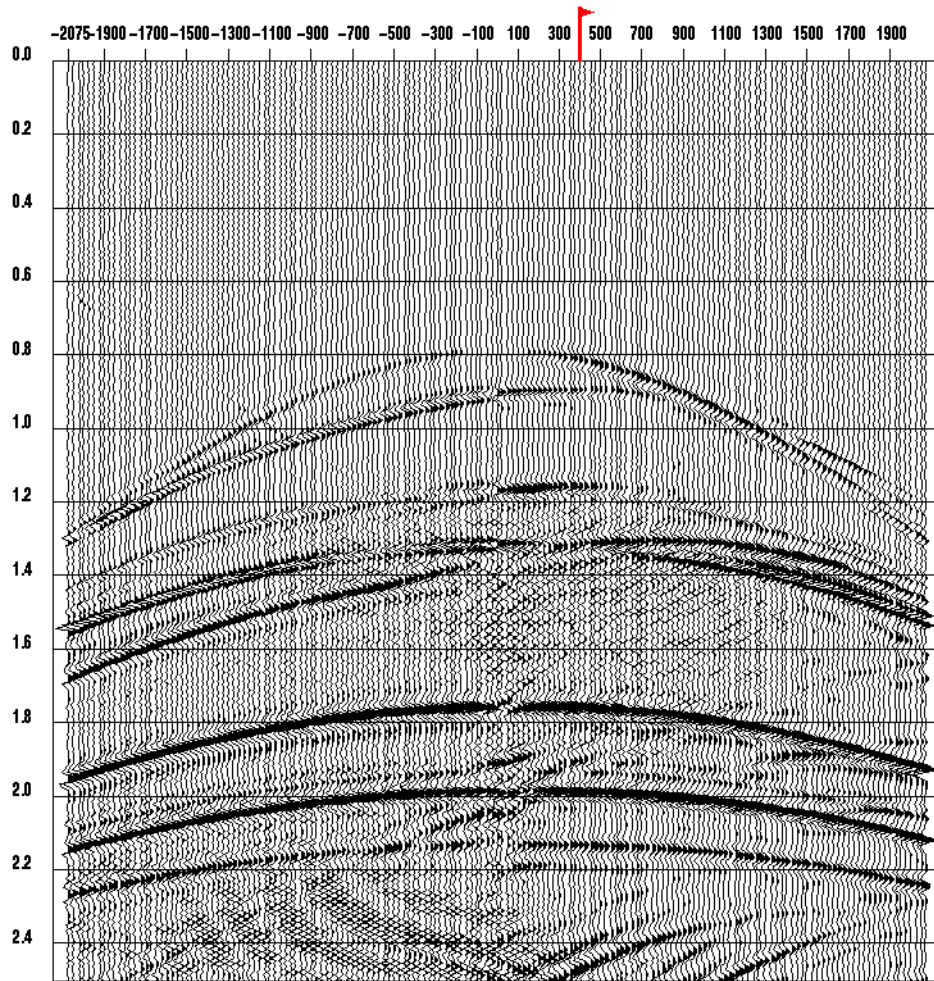


Fig. 19. Same as Figure 18, but with smaller offset range.

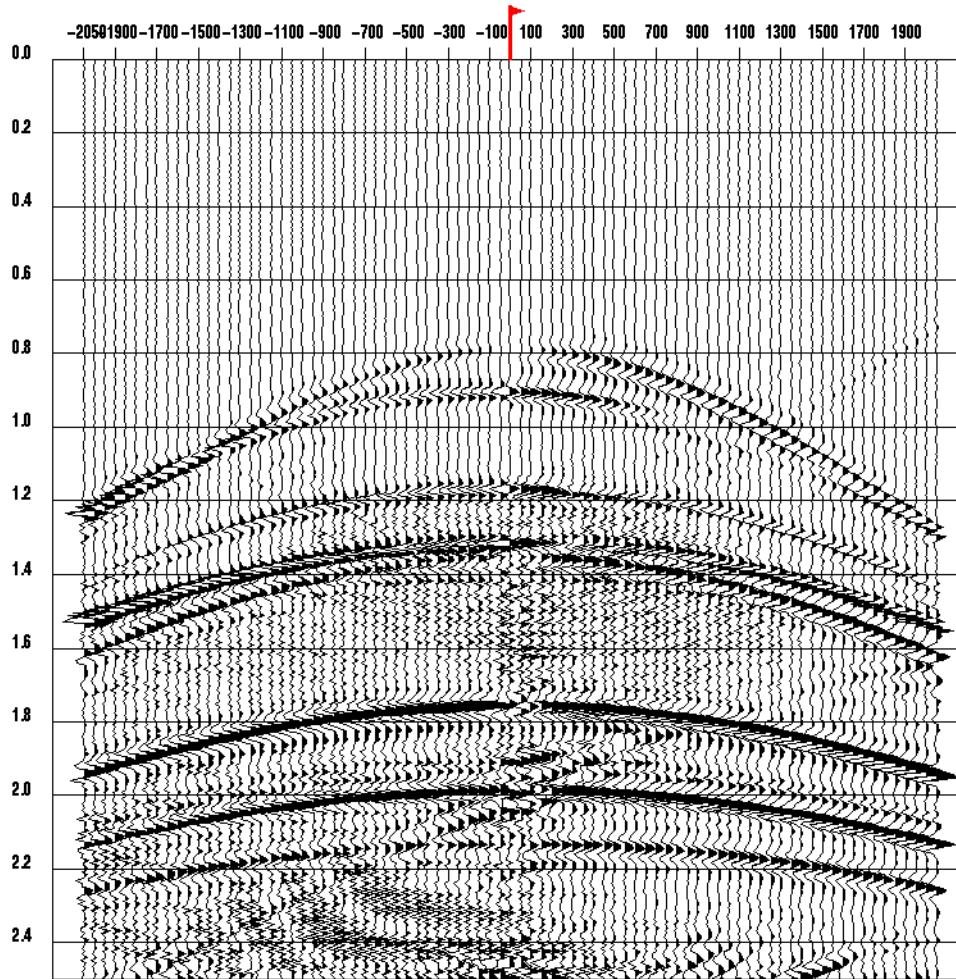


Fig. 20. The pseudo P-P CMP gather at station 1200. The reflection from the second layer becomes symmetric.

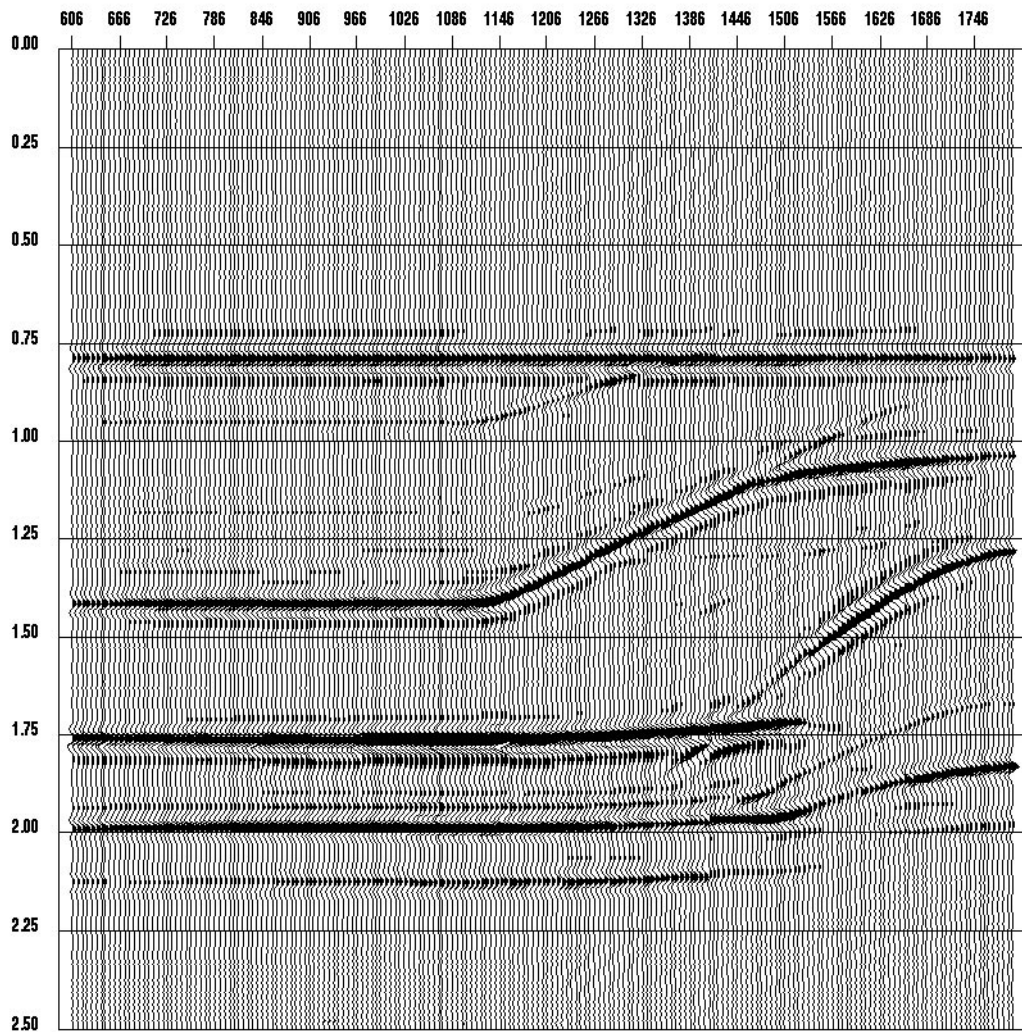


Fig. 21. Pseudo P-P DMO stack using the estimated V_p/V_s ratios from the result of simulated annealing. The times of the events match well with the true P-P DMO stack, except a slight mismatch of the layer occurs at station around 1606.

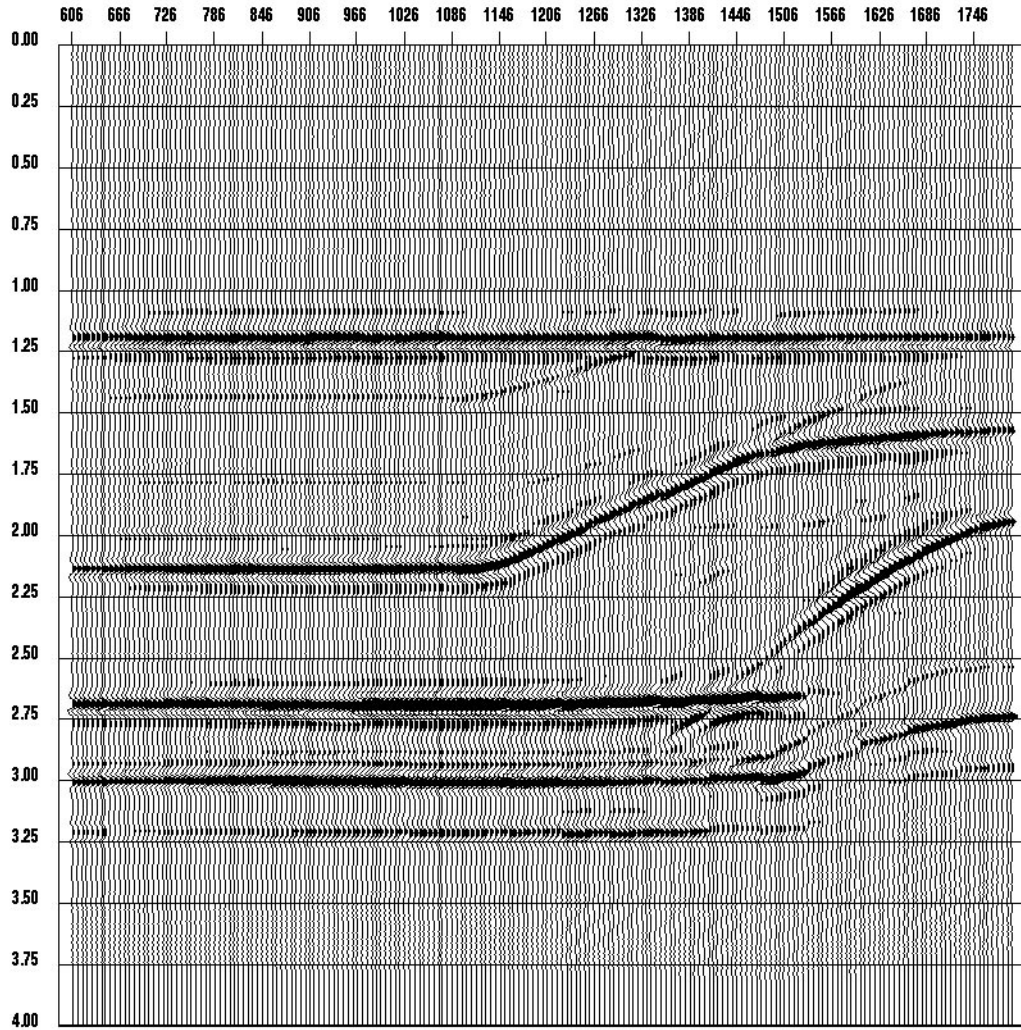


Fig. 22. The Pseudo P-P DMO stack of Figure 15 in P-S time. It is vertically stretched with the estimated V_p/V_s ratios. This stack also represents P-S DMO stack.

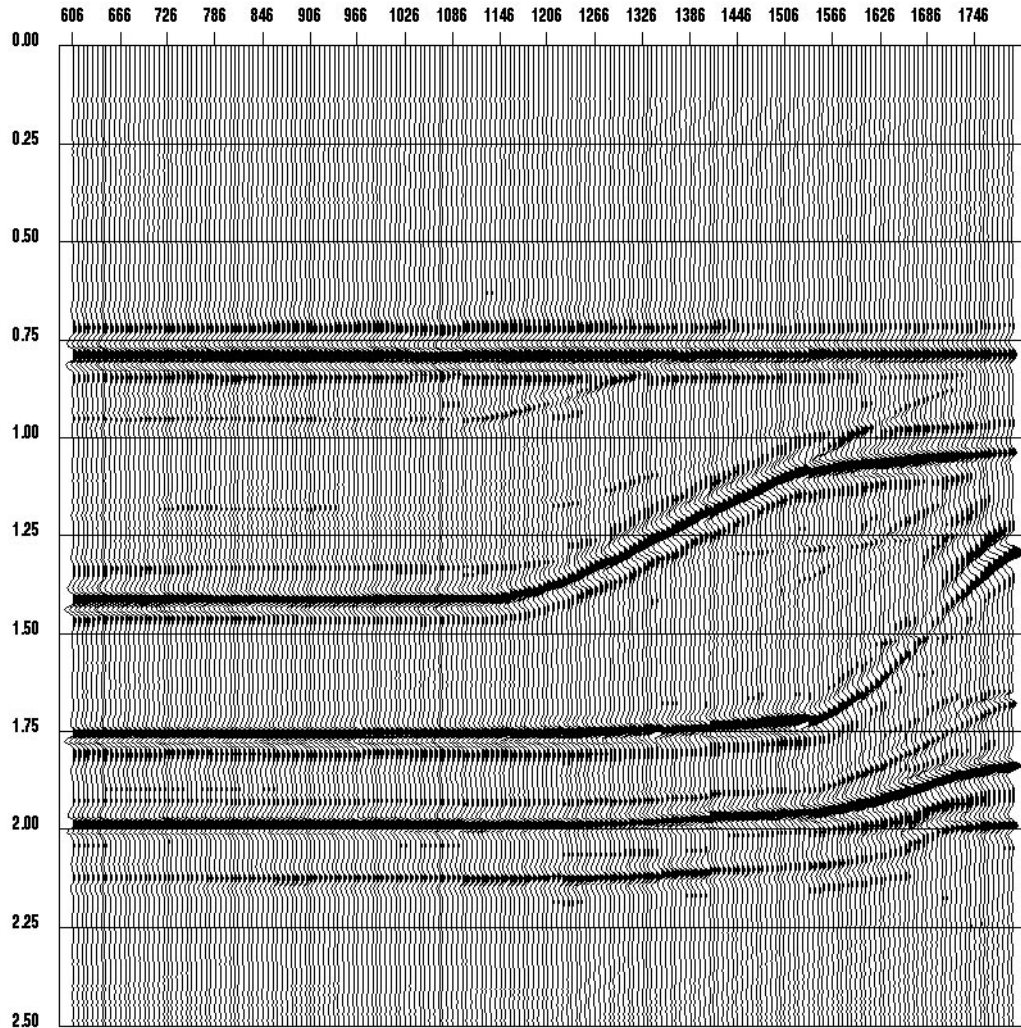


Fig. 23. The pseudo P-P prestack time migrated stack. The events closely match with those in Figure 12, the true P-P time migrated stack.

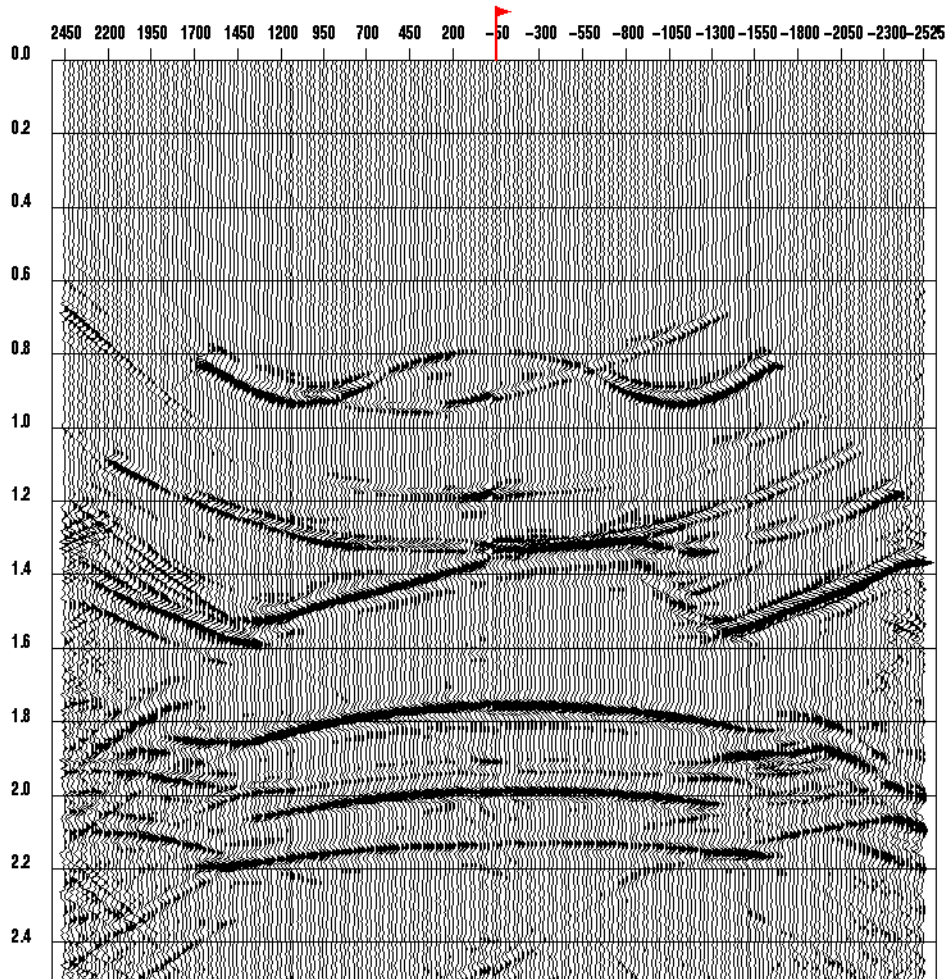


Fig. 24. The pseudo P-P receiver gather at station 1194. The ASMO is applied in receiver domain. Note that the valid offset of the events is less than the original input.

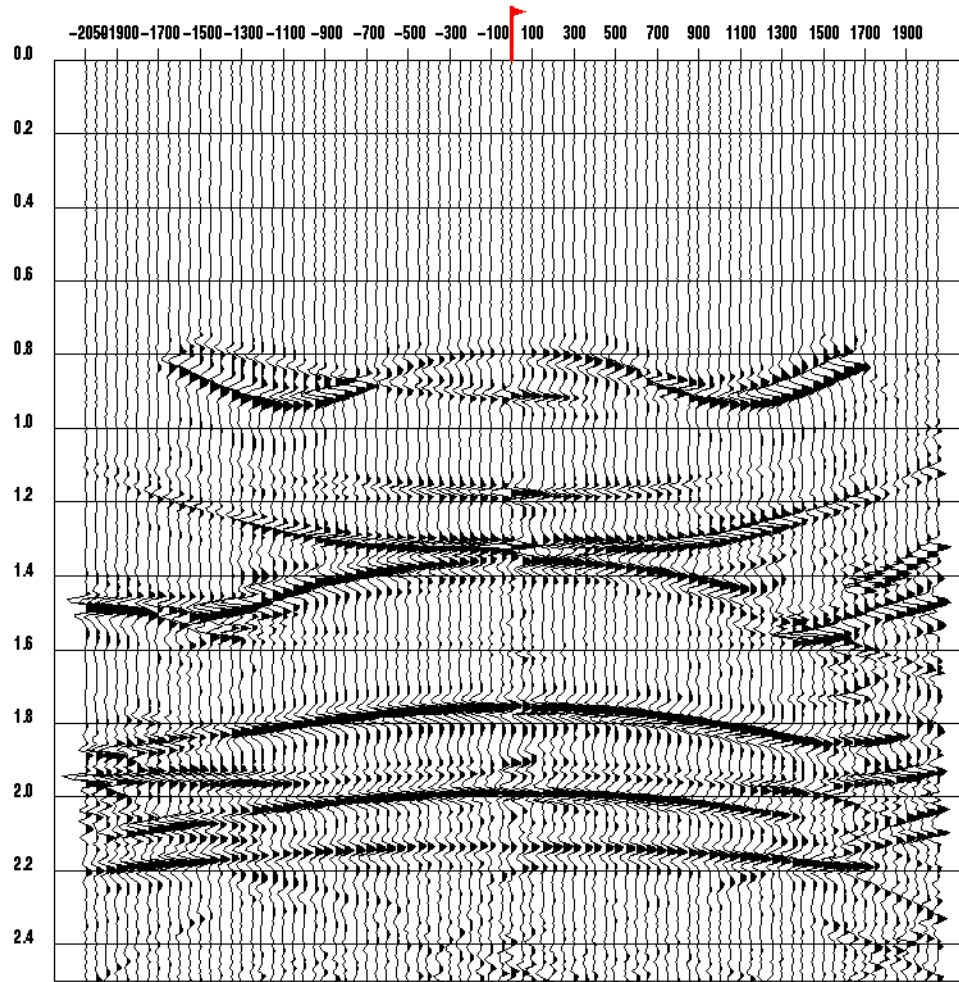


Fig. 25. The pseudo P-P CMP gather. The ASMO is applied in receiver domain. It

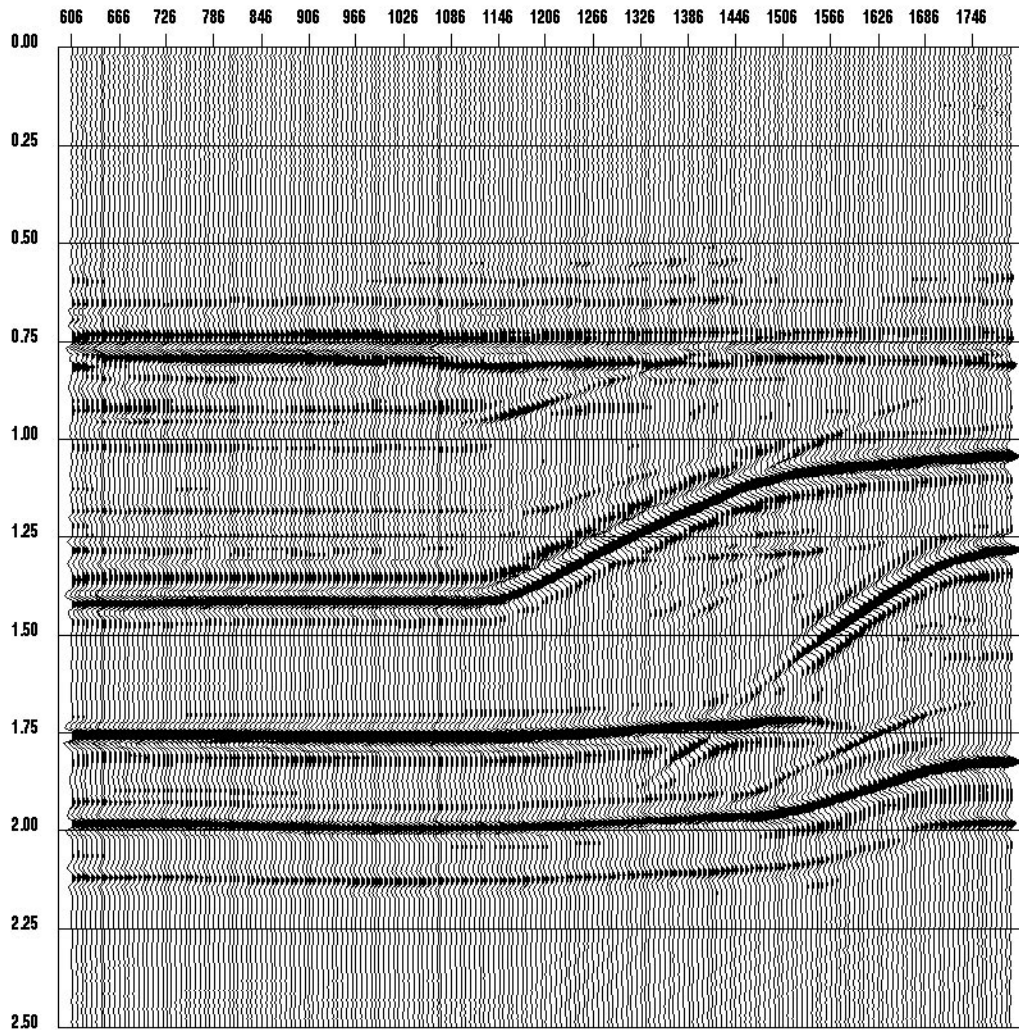


Fig. 26. The pseudo P-P DMO stack with the transformation applied in receiver domain. Fig. 9. A P-P CMP gather at station 1200. It is noted that the dipping event at 1.35 seconds is symmetric with respect to the offset.